World Journal of Applied Physics
2017; 2(3): 71-76
http://www.sciencepublishinggroup.com/j/wjap
doi: 10.11648/j.wjap.20170203.12

The Effect of Cladding Creep on the Initiation of GTRFW

William Richard Campbell*, Jerry Chen

Engineering Research Institute, Auckland University of Technology, Auckland, New Zealand

Email address:

williamcampbell.aut@gmail.com (W. R. Campbell)

*Corresponding author

To cite this article:

William Richard Campbell, Jerry Chen. The Effect of Cladding Creep on the Initiation of GTRFW. *World Journal of Applied Physics*. Vol. 2, No. 3, 2017, pp. 71-76. doi: 10.11648/j.wjap.20170203.12

Received: July 20, 2017; **Accepted**: September 5, 2017; **Published**: September 6, 2017

Abstract: Creep plays a critical role in the stress relaxation of a PWR fuel assembly, which causes the initiation of slip and fretting wear. In this paper, the creep down of grid and cladding is simulated using a 3D FEA model. A mechanism-based creep model is incorporated in the structural analysis. The evolution of stress as well as its effects on the slip and wear is analyzed. It is found the creep would lead to partial slip around the contact edge and eventually full slip across the entire contact interface. The contact stress and hydrostatic pressure in the water play key roles in the creep evolution.

Keywords: Wear, PWR, Creep, Zircaloy 4

1. Introduction

Creep is time dependent plastic deformation under the influence of stress and high temperature [1-5]. Depending on the temperature and stress level, there are several mechanisms of creep models. Frost and Ashby constructed deformation mechanism maps showing the dependence of plastic behavior on the temperature and stress [4]. Generally, under low temperature, dislocation glide dominates the plasticity. Under high stress level, power-law creep by dislocation glide, or glide-plus-climb is the major mechanism. Under high temperature, diffusional flow becomes the major mechanism. Although empirical models often used to describe the dependence of creep strain rate on the stress and temperature, mechanism based models are more reasonable due to their capability to reveal the physics of a material.

Creep may lead to failure to many engineering applications [1, 2, 6-27]. Predicting creep around a contact interface is mathematically challenging due to the possible involvement of relative motion [28-32]. Creep is an important factor that leads to the grid to rod fretting wear problem in a pressurized water reactor (PWR) [33-38]. In a PWR, a fuel rod is supported by preloaded springs and dimples on the spacer grid. The spacer grid and fuel rod cladding are made of Zircaloy due to its low absorption of thermal neutrons and corrosion resistance. Due to high temperature and stress, creep of Zircaloy causes stress relaxation. The insufficient support force would then lead to relative motion and wear on the grid to rod contact interface, eventually causes costly failure of the fuel rods.

Significant efforts have been made to study the stress relaxation on the contact interface between cladding and the spacer grid. Kim et al, used test rigs to experimentally analyze the loss of spring force and identified the key factors on the stress relaxation [34-36, 39-43]. Rubio et al developed a framework allowing the incorporation of creep with other physics such as vibrations and wear [44-46]. Pu et al. innovatively developed a diffusion-coupled cohesive zone model to capture the stress-assisted diffusional process along grain boundaries [17, 47]. Through experiments, significant efforts have been made by them to understand the behavior of alloy 617 under elevated temperature [48-50]. Wang et al, developed and validated a mechanism based creep model of Zircaloy based on large spectrum of experimental data, allowing reliable creep modeling under large range of temperature and stress [37, 38, 51]. Significant progress was also made by Hu et al. to study the wear propagation. The effects of shear strength and plasticity well explain the initiation and propagation of fretting wear [52-54]. They also developed an algorithm to efficiently couple wear and creep in a FEA model, allowing efficient and reliable simulation of the two mechanisms in GTRFW studies [33, 53-55].

In this paper, the creep down of the cladding and spacer grid is modeled using a 3D FEA model. A mechanism based creep model that has been validated in many experimental data is applied. The evolution of contact force and stress due to the creep is analyzed. Of particular interest is how the

creep affects the initiation and propagation slip behavior on the grid to rod interface.

2. Methodology

2.1. Creep Model

In a PWR, the pressure is maintained around 15MPa by a pressurizer in order to maintain a relatively high boiling point. Under such condition, the temperature of the coolant flow may reach 500-600k. The preload and the hydrostatic pressure from the coolant induce relative high stress in the fuel assembly. Due to the high temperature and stress, the creep deformation becomes significant over time. Many models have been developed to describe the dependence of creep rate on the stress and temperature in Zircaloy. Wang et al. developed a mechanism based creep model that has been validated by various experimental data and is capable to reflect the microscopic physics of Zircaloy [37]. In this article, this mechanism based model is adopted. Depending on the stress and temperature level, different creep mechanisms would dominate the plastic strain growth. When both the stress level is relatively low, diffusion or coble creep dominates the deformation. And the equation is as follows,

$$\dot{\gamma} = \frac{1.8\times10^{-3}}{Td^3}\tilde{\tau}\exp\left(-\frac{Q}{RT}\right), \quad (1)$$

where T is the temperature, d is the grain size and Q is the activation energy for diffusion.

When the stress level is relatively high, the dislocation glide creep becomes the dominant mechanism, and the creep rate is described by,

$$\dot{\gamma}_g = 10^{11}\exp\left[-\frac{175\pm5\times10^3}{RT}\left(1-\frac{\tilde{\tau}}{460}\right)\right]/s, \quad (2)$$

where τ is in MPa.

When the temperature level is relatively high, the power law creep dominates the creep growth, and the equation is,

$$\dot{\gamma}_p = \frac{8\times10^{11}G}{T}\left[\sinh\left(\frac{370\tilde{\tau}}{G}\right)\right]^{5.1}\exp\left[\frac{275\times10^3}{RT}\right]. \quad (3)$$

Wang et al. developed the model that is capable to automatically capture the creep rate without determining the dominant creep mechanism [37, 38].

2.2. FEA Model

A 3D model is constructed in Abaqus. The dimensions and boundary conditions are similar to a peer project. The simulation of creep deformation is computationally expensive, therefore, the details of the spacer grid is not modeled. The support from the spacer grid is equivalently represented by force springs. Both the cladding and springs are Zircaloy-4 with properties listed in Table 1. A uniform temperature of 600K is assumed in the model. During the simulation, a displacement of 100μm toward the central line of the cladding is applied to the springs so that the cladding is supported by a preload. Then the creep is switched on for certain time. A small axial displacement of 0.5μm is applied to the fuel rod after certain time of creep simulation to check if the contact force is still large enough to support the cladding against relative motion.

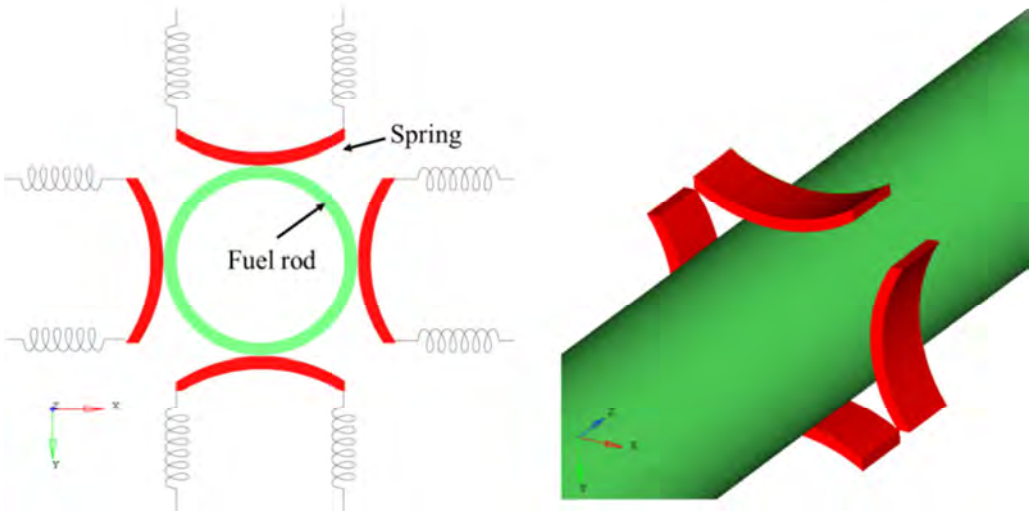

Figure 1. *A simplified with a fuel rod supported by a simplified spacer grid.*

Table 1. *Key parameters of the FEA model.*

Cladding thickness	0.57mm
Cladding diameter	9.5mm
Rod length (2 spans)	150mm
Density of Zircaloy 4	6.5×10^{-3} g/mm³
Young's modulus of Zircaloy 4	75GPa
Poisson's ratio of Zircaloy 4	0.37

3. Results

The major effect of creep in a PWR fuel assembly is stress relaxation, which eventually lead to wear on the cladding surface. The operation time of a fuel assembly is expected to be as long as years. Even though creep is a relatively slow process, the cumulative creep strain over such long time is

pretty considerable and will cause significant stress relaxation. Figure 2 shows the creep strain on the cladding. The creep basically concentrates around the contact contour. The strain has two peak area because the deflection of the spring leads to two high stress areas.

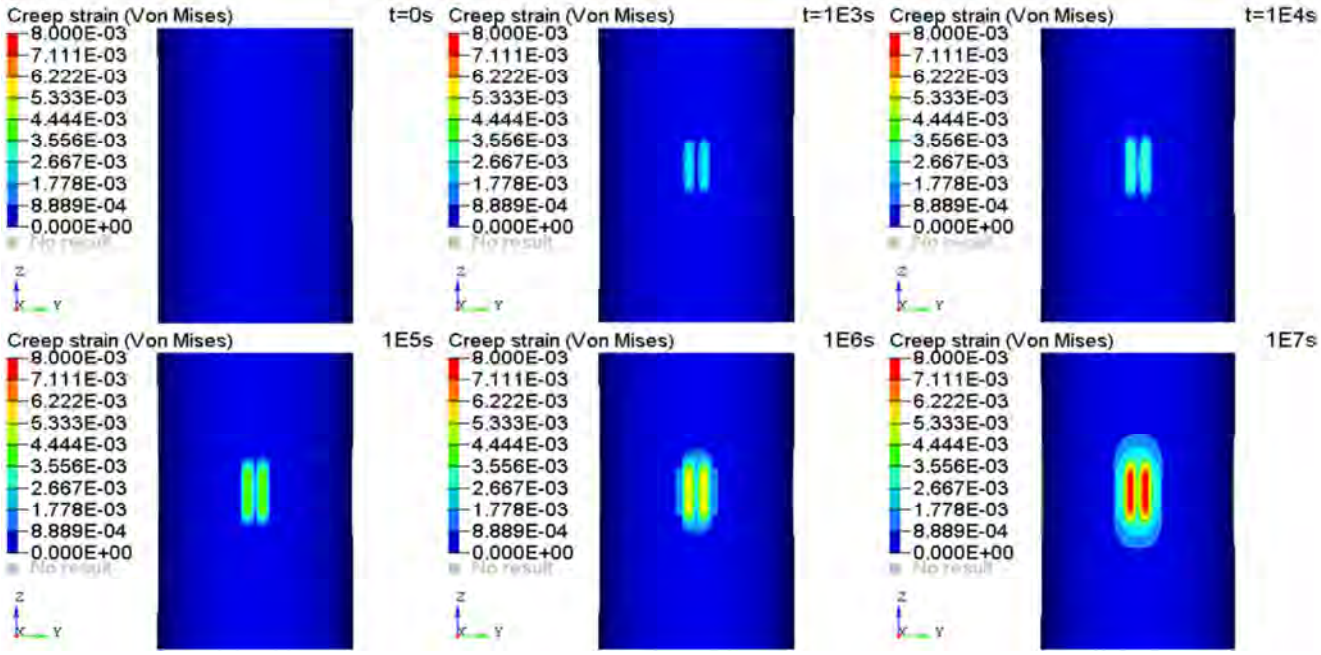

Figure 2. *Creep strain grows over time and concentrates around the contact contour between the springs and cladding.*

The normal contact force represents the amount of support on cladding against wear. Figure 3 shows the evolution of normal contact force over time. As the creep grows, the normal contact force decreases. It is noticed that the contact force decreases rapidly at the beginning due to high initial stress level. As the stress level drops, the contact force decreases slower. It is expected to reach a limit at which the creep growth is negligible. As the contact force drops, it becomes easier for an external force to overcome the static frictional force and cause relative motion. When the contact force is small enough, the external force and vibration can even cause separation between the spring and the cladding.

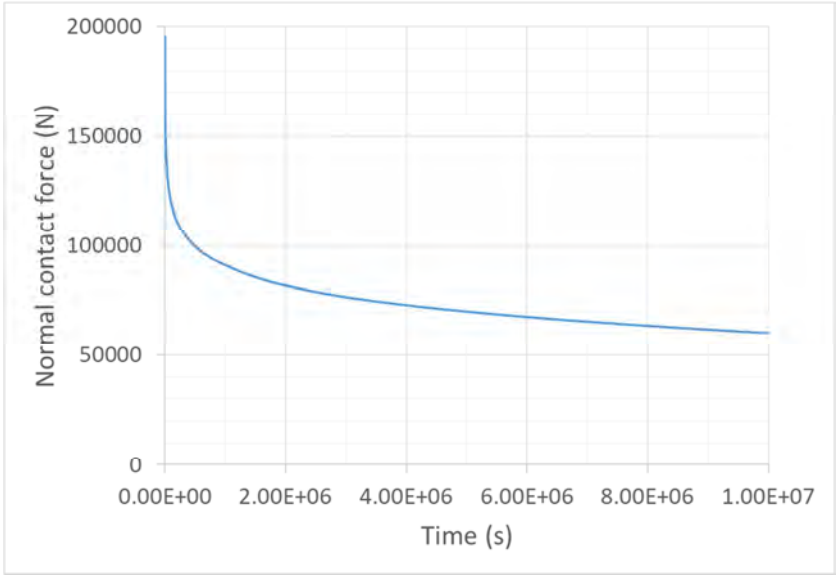

Figure 3. *The normal contact force decreases as the creep grows. The force decreases rapidly at the early stage since the stress level is high.*

The slip is directly related to the wear growth on the cladding, therefore, the relationship between creep and slip is critical to determine how the creep affect the initiation of wear. Figure 4 shows the distribution of slip distance after certain time of creep simulation. In this study, a static friction coefficient of 0.15 and a dynamic friction coefficient of 0.1 are assumed. The slip distance is normalized by the axial displacement. At the beginning, only micro slip is noticed

around the contact edge between the cladding and spring. As the creep grows, the contact force drops and leads to a decreased static friction force. In this scenario, the partial slip propagates to the entire contact surface. Due to the increased slip distance, the grow rate of the GTRFW increased significantly as well. Therefore, creep is accounted a major cause of GTRFW initiation. Such phenomenon is consistent with the observations by Hu and Wang et al [38, 53-55].

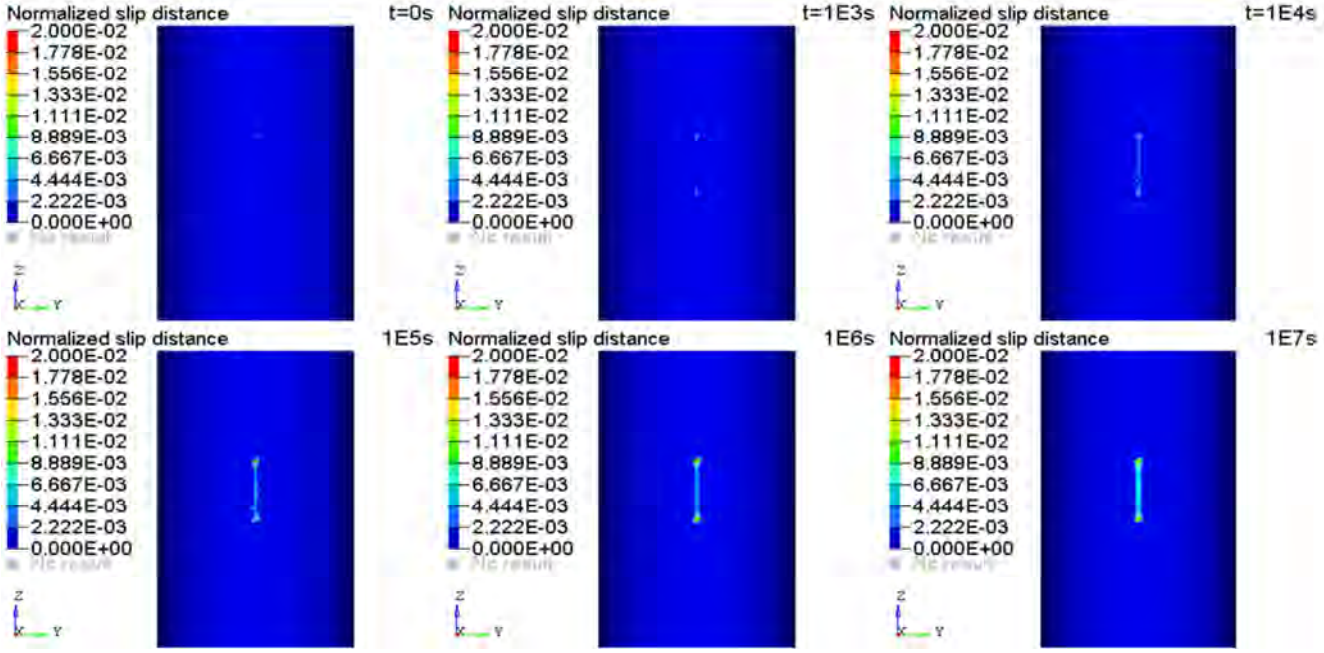

Figure 4. *The slip distance increases with the creep strain: when the creep is small, only micro partial slip is noticed around the contact edges, as the creep grows, the slip propagates to the entire contact interface.*

4. Conclusions

In this paper, the evolution of creep has been modeled in a 3D FEA model using a mechanism based creep model. The effects of the creep on the initiation of slip was analyzed. It is found that both the contact stress and the hydrostatic pressure from the coolant play important roles in the creep deformation. Due to the stress relaxation caused by creep, partial slip is first observed around the edge of the springs. Eventually, the slip propagates to the entire contact contour. This well explained the experimental observations in previous studies and is consistent with theoretical results.

References

[1] Woodford, D. A., Creep analysis of zircaloy-4 and its application in the prediction of residual stress relaxation. Journal of Nuclear Materials, 1979. 79 (2): p. 345-353.

[2] Jacobs, O., et al., Creep and wear behaviour of ethylene–butene copolymers reinforced by ultra-high molecular weight polyethylene fibres. Wear, 2002. 253 (5–6): p. 618-625.

[3] Bassani, J. L. and F. A. McClintock, Creep relaxation of stress around a crack tip. International Journal of Solids and Structures, 1981. 17 (5): p. 479-492.

[4] Frost, H. J. and M. F. Ashby, Deformation Mechanism Maps: The Plasticity and Creep of Metals and Ceramics. 1982, Oxford, UK: Pergamon Press.

[5] Was, G. S., Irradiation Creep and Growth, in Fundamentals of Radiation Materials Science: Metals and Alloys. 2007, Springer Berlin Heidelberg: Berlin, Heidelberg. p. 711-763.

[6] Ma, X., et al., In-situ observations of the effects of orientation and carbide on low cycle fatigue crack propagation in a single crystal superalloy. Procedia Engineering, 2010. 2 (1): p. 2287-2295.

[7] Ma, X., et al., Temperature effect on low-cycle fatigue behavior of nickel-based single crystalline superalloy. Acta Mechanica Solida Sinica, 2008. 21 (4): p. 289-297.

[8] Ma, X. and H.-J. Shi, On the fatigue small crack behaviors of directionally solidified superalloy DZ4 by in situ SEM observations. International Journal of Fatigue, 2012. 35 (1): p. 91-98.

[9] Wei, C., J. Chan, and D. Garmire. 3-axes MEMS Hall-effect sensor. in Sensors Applications Symposium (SAS), 2011 IEEE. 2011.

[10] Wei, C. and L. L. Gouveia, Modeling and simulation of Maximum power point tracker in Ptolemy. Journal of Clean Energy Technologies, 2013. 1 (1): p. 6-9.

[11] Wei, C. and F. Shi, High Performance SOI RF Switch for Healthcare Application. International Journal of Enhanced Research in Science, Technology & Engineering, 2016. 5 (10): p. 23-28.

[12] Wei, C., J. Xu, and S. Wang, Low Power SI Class E Power Amplifier for Healthcare Application. International Journal of Electronics Communication and Computer Engineering, 2016. 7 (6): p. 290-293.

[13] He, J. and Y. Fuh-Gwo, A quantitative damage imaging technique based on enhanced CCRTM for composite plates using 2D scan. Smart Materials and Structures, 2016. 25 (10): p. 105022.

[14] He, J. and F.-G. Yuan, Damage identification for composite structures using a cross-correlation reverse-time migration technique. Structural Health Monitoring, 2015. 14 (6): p. 558-570.

[15] He, J. and F.-G. Yuan, Lamb-wave-based two-dimensional areal scan damage imaging using reverse-time migration with a normalized zero-lag cross-correlation imaging condition. Structural Health Monitoring, 2016: p. 1475921716674373.

[16] He, J. and F.-G. Yuan, Lamb wave-based subwavelength damage imaging using the DORT-MUSIC technique in metallic plates. Structural Health Monitoring, 2016. 15 (1): p. 65-80.

[17] Pu, C. and Y. Gao, Crystal Plasticity Analysis of Stress Partitioning Mechanisms and Their Microstructural Dependence in Advanced Steels. Journal of Applied Mechanics, 2015. 82 (3): p. 031003-031003-6.

[18] Li, W., et al., Cell Wall Buckling Mediated Energy Absorption in Lotus-type Porous Copper. Journal of Materials Science & Technology, 2015. 31 (10): p. 1018-1026.

[19] Sun, Z., et al., Load partitioning between the bcc-iron matrix and NiAl-type precipitates in a ferritic alloy on multiple length scales. 2016. 6: p. 23137.

[20] Li, H., et al. Application of Artificial Neural Networks in predicting abrasion resistance of solution polymerized styrene-butadiene rubber based composites. in 2014 IEEE Workshop on Electronics, Computer and Applications. 2014.

[21] Liu, Z., et al., Design of high-performance water-in-glass evacuated tube solar water heaters by a high-throughput screening based on machine learning: A combined modeling and experimental study. Solar Energy, 2017. 142: p. 61-67.

[22] Liu, Z., et al., Novel Method for Measuring the Heat Collection Rate and Heat Loss Coefficient of Water-in-Glass Evacuated Tube Solar Water Heaters Based on Artificial Neural Networks and Support Vector Machine. Energies, 2015. 8 (8): p. 8814.

[23] Li, H., et al., Comparative Study on Theoretical and Machine Learning Methods for Acquiring Compressed Liquid Densities of 1,1,1,2,3,3,3-Heptafluoropropane (R227ea) via Song and Mason Equation, Support Vector Machine, and Artificial Neural Networks. Applied Sciences, 2016. 6 (1): p. 25.

[24] Kim, T., et al., Hybrid tandem quantum dot/organic photovoltaic cells with complementary near infrared absorption. Applied Physics Letters, 2017. 110 (22): p. 223903.

[25] Wolf, J., et al., Benzo [1,2-b:4,5-b′]dithiophene–Pyrido [3,4-b]pyrazine Small-Molecule Donors for Bulk Heterojunction Solar Cells. Chemistry of Materials, 2016. 28 (7): p. 2058-2066.

[26] Wang, K., et al., Donor and Acceptor Unit Sequences Influence Material Performance in Benzo [1,2-b:4,5-b′]dithiophene–6,7-Difluoroquinoxaline Small Molecule Donors for BHJ Solar Cells. Advanced Functional Materials, 2016. 26 (39): p. 7103-7114.

[27] Liang, R.-Z., et al., Benzo [1,2-b:4,5-b′]Dithiophene–6,7-Difluoroquinoxaline Small Molecule Donors with >8% BHJ Solar Cell Efficiency. Advanced Energy Materials: p. 1602804-n/a.

[28] Xu, Q., et al., Robust self-cleaning and micromanipulation capabilities of gecko spatulae and their bio-mimics. 2015. 6: p. 8949.

[29] Xu, Q., et al., Three-dimensional micro/nanoscale architectures: fabrication and applications. Nanoscale, 2015. 7 (25): p. 10883-10895.

[30] Xu, Q., et al., Dynamic Adhesion Forces between Microparticles and Substrates in Water. Langmuir, 2014. 30 (37): p. 11103-11109.

[31] Xu, Q., et al., Dynamic Enhancement in Adhesion Forces of Microparticles on Substrates. Langmuir, 2013. 29 (45): p. 13743-13749.

[32] Teeter, M. G., et al., Wear and Creep Behavior of Total Knee Implants Undergoing Wear Testing. The Journal of Arthroplasty, 2015. 30 (1): p. 130-134.

[33] Hu, Z., M. D. Thouless, and W. Lu, Effects of gap size and excitation frequency on the vibrational behavior and wear rate of fuel rods. Nuclear Engineering and Design, 2016. 308: p. 261-268.

[34] Kim, K.-T., The study on grid-to-rod fretting wear models for PWR fuel. Nuclear Engineering and Design, 2009. 239 (12): p. 2820-2824.

[35] Kim, K.-T., A study on the grid-to-rod fretting wear-induced fuel failure observed in the 16×16KOFA fuel. Nuclear Engineering and Design, 2010. 240 (4): p. 756-762.

[36] Kim, K.-T. and J.-M. Suh, Development of an advanced PWR fuel for OPR1000s in Korea. Nuclear Engineering and Design, 2008. 238 (10): p. 2606-2613.

[37] Wang, H., et al., A mechanism-based framework for the numerical analysis of creep in zircaloy-4. Journal of Nuclear Materials, 2013. 433 (1–3): p. 188-198.

[38] Wang, H., et al., The effect of coupled wear and creep during grid-to-rod fretting. Nuclear Engineering and Design, 2017. 318: p. 163-173.

[39] Kim, K. and J. Suh, Impact of nuclear fuel assembly design on grid-to-rod fretting wear. Journal of Nuclear Science and Technology, 2009. 46: p. 149–157.

[40] Kim, K.-T., The effect of fuel rod loading speed on spacer grid spring force. Nuclear Engineering and Design, 2010. 240 (10): p. 2884-2889.

[41] Kim, K.-T., The effect of fuel rod supporting conditions on fuel rod vibration characteristics and grid-to-rod fretting wear. Nuclear Engineering and Design, 2010. 240 (6): p. 1386-1391.

[42] Kim, K.-T., Applicability of out-of-pile fretting wear tests to in-reactor fretting wear-induced failure time prediction. Journal of Nuclear Materials, 2013. 433 (1–3): p. 364-371.

[43] Kim, K.-T. and J.-M. Suh, Impact of nuclear fuel assembly design on grid-to-rod fretting wear. Journal of Nuclear Science and Technology, 2009. 46 (2): p. 149-157.

[44] Rubiolo, P. R., Probabilistic prediction of fretting-wear damage of nuclear fuel rods. Nuclear Engineering and Design, 2006. 236 (14–16): p. 1628-1640.

[45] Rubiolo, P. R. and M. Y. Young, VITRAN: an advance statistic tool to evaluate fretting-wear damage. Journal of Power and Energy Systems, 2008. 2 (1): p. 57-66.

[46] Rubiolo, P. R. and M. Y. Young, On the factors affecting the fretting-wear risk of PWR fuel assemblies. Nuclear Engineering and Design, 2009. 239 (1): p. 68-79.

[47] Pu, C., et al., Diffusion-coupled cohesive interface simulations of stress corrosion intergranular cracking in polycrystalline materials. Acta Materialia, 2017. 136: p. 21-31.

[48] Sham, S., et al., Report on FY15 alloy 617 code rules development. 2015: United States.

[49] Wang, Y., et al., Report on FY15 Alloy 617 SMT Creep-Fatigue Test Results. 2015; Oak Ridge National Laboratory (ORNL). p. Medium: ED; Size: 56 p.

[50] Wang, Y., et al., Report on FY15 Two-Bar Thermal Ratcheting Test Results. 2015, ; Oak Ridge National Lab. (ORNL), Oak Ridge, TN (United States). p. Medium: ED; Size: 39 p.

[51] Lu, W., et al., CASL Structural Mechanics Modeling of Grid-to-Rod Fretting (GTRF). JOM, 2016. 68 (11): p. 2922-2929.

[52] Hu, Z., et al., Simulation of wear evolution using fictitious eigenstrains. Tribology International, 2015. 82, Part A (0): p. 191-194.

[53] Hu, Z., W. Lu, and M. D. Thouless, Slip and wear at a corner with Coulomb friction and an interfacial strength. Wear, 2015. 338–339: p. 242-251.

[54] Hu, Z., et al., Effect of plastic deformation on the evolution of wear and local stress fields in fretting. International Journal of Solids and Structures, 2016. 82: p. 1-8.

[55] Hu, Z., Contact around a Sharp Corner with Small Scale Plasticity. Advances in Materials, 2017. 6 (1): p. 10-17.